Coordination Chemistry Reviews 255 (2011) 1981–1990

Contents lists available at ScienceDirect

Coordination Chemistry Reviews

journal homepage: www.elsevier.com/locate/ccr

Review

Spin-crossover in cobalt(II) compounds containing terpyridine and its derivatives

Shinya Hayami*, Yasuka Komatsu, Tetsuya Shimizu, Hidenobu Kamihata, Young Hoon Lee

Department of Chemistry, Graduate School of Science and Technology, Kumamoto University, 2-39-1 Kurokami, Kumamoto, Japan

Contents

ARTICLE INFO

Article history:
Received 18 February 2011
Accepted 25 May 2011
Available online 7 July 2011

Keywords:
Spin-crossover
Cobalt(II) complexes
Terpyridine
Soft materials

ABSTRACT

In this review article we discuss the unique and novel magnetic properties for the cobalt(II) compounds with a variety of terpy derivatives including substituents at the 4-position. These are also compared with the unsubstituted terpy cobalt(II) complex. Since the first SCO cobalt(II) complex with terpy ligand was reported, this system has been widely studied. SCO cobalt(II) complexes possessing terpy or OH-terpy ligand reveal incomplete or gradual SCO behavior. The pyterpy-appended cobalt(II) complex shows SCO depending on the guest molecules involved. Cobalt(II) complexes with long-alkylated terpy ligands, $[Co(Cn\text{-terpy})_2](BF_4)_2$ (n = 16, 14 and 12) have been synthesized and some were characterized by single crystal X-ray analysis. Furthermore, variable-temperature magnetic susceptibility indicated that the non-solvated compounds $[Co(Cn\text{-terpy})_2](BF_4)_2$ (n = 16, 14 and 12) exhibit "reverse spin transition" phenomenon with wide thermal hysteresis around room temperature. In addition, the solvated compound $[Co(C12\text{-terpy})_2](BF_4)_2{\cdot}EtOH{\cdot}0.5H_2O$ shows "re-entrant SCO" behavior. The long alkyl chains in SCO cobalt(II) complexes can lead to novel physical properties resulting from a synergetic effect between SCO and response of the flexibility toward external stimuli.

1. Introduction

Metal complexes with configurations of d^4 to d^7 electrons may exist in either the high-spin (HS) or low-spin (LS) states depending on the nature of the ligand field strength. When the ligand field strength is weak, the electronic ground state is HS where the spin multiplicity becomes a maximum. On the other hand, when the strength is strong, the ground state stabilizes in the LS state with minimum multiplicity. When the ligand field strength is close to the crossover point between HS and LS states, the interconversion between HS and LS states, called as spin-crossover (SCO), can be reversibly induced by external stimuli (temperature, pressure, a magnetic field, an electric field, and light). Since Cambi first observed the SCO phenomenon for tris(dithiocarbamato)iron(III) complexes as the spin isomers in 1931 [1], it has often been found in the complexes of iron(II), iron(III) and cobalt(II) [2]. The SCO spin transition curves exhibit various forms in the solid state because of long-range cooperative interactions. In particular, a large number of SCO iron(II) and iron(III) complexes have been studied due to the availability of Mössbauer spectroscopy [3–11]. In comparison with iron(II) or iron(III) SCO complexes, only a few cobalt(II) complexes with SCO behavior are known until now [12–27]. In the solid

* Corresponding author. Tel.: +81 96 342 3469; fax: +81 96 342 3469.
E-mail address: hayami@sci.kumamoto-u.ac.jp (S. Hayami).

0010-8545/$ – see front matter © 2011 Elsevier B.V. All rights reserved.
doi:10.1016/j.ccr.2011.05.016

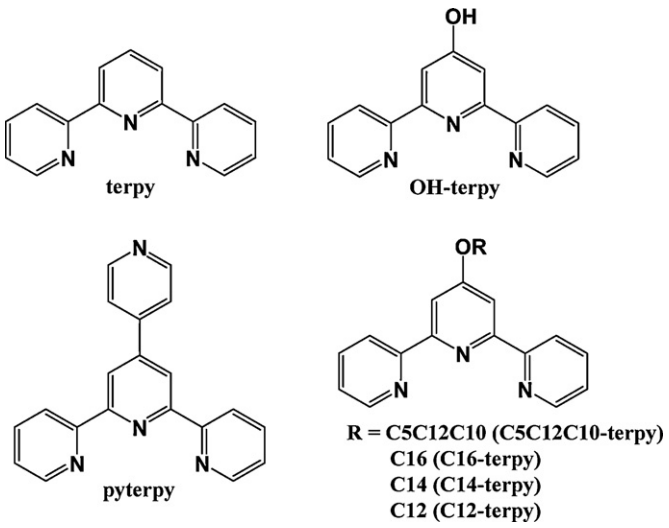

Scheme 1. The chemical structure of terpy derivatives considered in this review.

state, cooperativity is worthy of consideration if intermolecular interactions are sufficiently strong. Cooperativity induces abrupt spin transitions and hysteresis loops in SCO compounds, which is the reason why the role of intermolecular interactions in spin transitions has been extensively studied. In this regard, the design of SCO compounds became one of the main challenges to exhibit large cooperativity. It has been also theoretically suggested and experimentally confirmed that cooperativity can be increased by designing polymeric structures in which the active sites are linked to each other by chemical bridges [28–33]. Indeed, SCO compounds forming strong intermolecular interactions, such as π–π stacking, hydrogen bonding, or interchain interaction, exhibit abrupt transitions and hysteresis loops [34–52]. The SCO compounds with cooperative effects have been focused on a rigid system so far. However we have been interested in flexible and soft SCO compounds, which could be synthesized by employing long alkyl chains to give interchain interaction between other side ligands. Interchain interactions caused by long alkyl chain lead to magnetically unique characteristics for cobalt(II) compounds, especially "reverse spin transition" and "re-entrant SCO". "Reverse spin transition" is defined as the spin transition from HS to LS states on heating and from LS to HS states on cooling, i.e. exhibiting an opposite spin transition phenomenon compared with that of typical SCO compounds. "Re-entrant SCO" is also defined as V-shape SCO (HS–LS–HS).

This review is specially focused on the intermolecular interaction of SCO cobalt(II) complexes with terpy (terpy = 2,2′:6′,2″-terpyridine) derivatives (Scheme 1), and their unique magnetic and structural features.

2. Spin-crossover cobalt(II) complexes

The SCO cobalt(II) compounds has been reviewed by Goodwin [2]. The SCO phenomenon for cobalt(II) complexes shows spin conversion between $S = 3/2$ ($t_{2g}^5e_g^2$) and $S = 1/2$ ($t_{2g}^6e_g^1$) spin states. The magnetic behavior is characterized by the temperature-dependent magnetic susceptibility which is measured in the form of the χ_mT versus T plots, where χ_m is the molar magnetic susceptibility and T is the temperature. For the SCO cobalt(II) complexes, the χ_mT value in the LS state is around 0.5 $cm^3\,K\,mol^{-1}$, whereas that in the HS state appears in the range of 1.9–3.5 $cm^3\,K\,mol^{-1}$ due to the contribution of the orbit angular momentum. Such a SCO involves one electron transfer from the t_{2g} to the e_g orbitals, in contrast to the similar process in iron(II) or iron(III) SCO complexes where two electron transfer occurs. This is the origin of several important differences in the feature of SCO between cobalt(II) complexes and iron(II) or iron(III) complexes. The significant difference is in the changes of distance between the metal and the coordinated donor atom (Δr_{HL}) accompanying SCO. The change of approximately ~0.10 Å, ~0.15 Å, and ~0.20 Å in Δr_{HL} takes place concomitantly with the SCO in cobalt(II), iron(III), and iron(II) complexes, respectively [2,3]. While the molecular volume changes with respect to the SCO in cobalt(II) is less pronounced than that in iron(II) or iron(III), it generally leads to the gradual SCO in cobalt(II) complexes in the vast majority of instances. The difference of the entropy based on SCO (ΔS_{spin}) can be expressed in the equation of $\Delta S_{spin} = R\ln[(2S+1)_{HS}/(2S+1)_{LS}]$, thus the value for the SCO cobalt(II) complexes ($\Delta S_{spin} = 5.8\,J\,K^{-1}\,mol^{-1}$) is smaller than those for SCO iron(II) ($\Delta S_{spin} = 13.38\,J\,K^{-1}\,mol^{-1}$) or iron(III) ($\Delta S_{spin} = 9.13\,J\,K^{-1}\,mol^{-1}$) complexes. Therefore, SCO cobalt(II) complexes show the spin conversion between HS and LS states with smaller external stimuli compared with iron(II) or iron(III) SCO complexes.

2.1. Spin-crossover cobalt(II) complexes with terpy ligand

Since the first SCO cobalt(II) complex, $[Co(terpy)_2]Br_2\cdot H_2O$ (terpy = 2,2′:6′,2″-terpyridine) was reported, SCO cobalt(II) complexes with a diversity of terpy derivatives as ligand exhibiting $S = 1/2 \leftrightarrow 3/2$ spin changes have been widely studied, (see Goodwin's review and the references therein [2,13,53–62]). The SCO cobalt(II) complexes, $[Co(terpy)_2]X_2\cdot nH_2O$ ($X = Br^-$, Cl^-, I^-, F^-, ClO_4^-, NCS^-, NO_3^-, $[Co(CN)_4]^{2-}$, SO_4^{2-}, BPh_4^-, and $n = 0$–6) show various SCO behavior generating incomplete or gradual SCO curves. The structural analyses for the various salts of $[Co(terpy)_2]^{2+}$ revealed that the predominant change occurs in $Co–N_{central}$ distance (~0.21 Å), while the change in $Co–N_{distal}$ distance accompanying SCO is only ~0.07 Å. Furthermore, the Jahn–Teller effect is operative in LS state because of a single e_g electron.

$[Co(terpy)_2](ClO_4)_2\cdot 0.5H_2O$ (**1·0.5H$_2$O**) serves as a good example to confirm the relationship between the bond lengths of metal–ligand and SCO behavior [60]. The compound **1·0.5H$_2$O** was crystallized in a tetragonal $P4(2)/n$ space group (Fig. 1). The cobalt(II) ions has pseudo-octahedral coordination geometry, and the six coordination sites are occupied by nitrogen atoms from the terpy ligand. The average distance of Co–N bonds between central/distal pyridines and metal ion for the HS state are $Co–N_{central} = 2.02$ Å and $Co–N_{distal} = 2.14$ Å, respectively. Temperature-dependent magnetic susceptibilities for the compound show that the χ_mT value at 322 K is equal to 2.30 $cm^3\,K\,mol^{-1}$, which corresponds to an expected value for the isolated HS cobalt(II) ion with $g = 2.022$, and then gradually decreases as the temperature is lowered, and more than 96% is converted into the LS state below ca. 80 K (Fig. 2).

The SCO cobalt(II) compound $[Co(terpy)_2](BF_4)_2$ (**2**) was also studied by variable-temperature crystallography [62]. The compound **2** retains the same space group(*Cc*) in the HS (375 K) and LS (30 K) state. The structure at 30 K shows a pronounced Jahn–Teller elongation along the N(27)–Co(1)–N(33) direction. The axial $Co–N_{central}$ distances (Co(1)–N(2) = 1.907(3) Å and Co(1)–N(20) = 1.925(2) Å) are shorter than $Co–N_{distal}$ distances (Co(1)–N(9) = 2.066(2) Å, Co(1)–N(15) = 2.066(2) Å, Co(1)–N(27) = 2.107(2) Å, and Co(1)–N(33) = 2.132(2) Å). This elongation is not observed at 100 K and beyond owing to the onset of dynamic disorder in the axis elongation between the Co–N bonds. Consistent with the result of susceptibility, the Co–N distances in the complex increase continuously upon warming from 100 to 300 K. Although the average Co–N distance is almost constant, the individual Co–N lengths between 300 and 375 K show more complicated variation with temperature change. The fundamental structure at 375 K

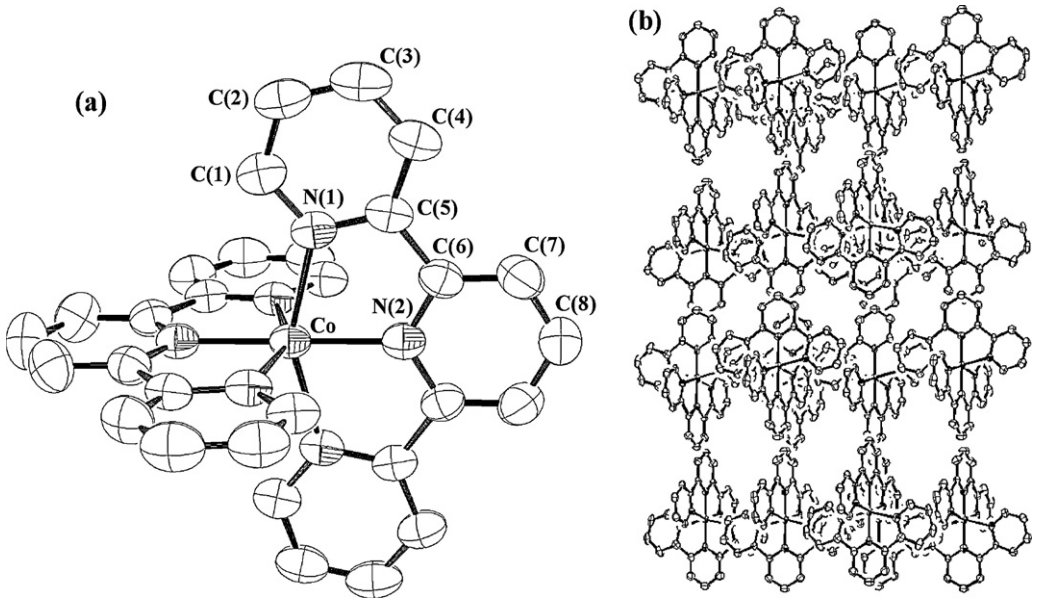

Fig. 1. (a) ORTEP drawing of cation of **1·0.5H$_2$O** showing 50% probability displacement ellipsoids. (b) Projection of the crystal structure of cation of **1·0.5H$_2$O** along the *bc* plane. ClO_4^- anions, H_2O molecules and H atoms are omitted for clarity.
Adapted from Ref. [60].

is similar to that in LS state except for bond distances and angles. The axial Co–$N_{central}$ distances (Co(1)–N(2) = 2.045(4) Å and Co(1)–N(20) = 2.030(4) Å) are shorter than Co–N_{distal} distances (Co(1)–N(9) = 2.160(3) Å, Co(1)–N(15) = 2.151(3) Å, Co(1)–N(27) = 2.149(3) Å, and Co(1)–N(33) = 2.156(3) Å). Magnetic susceptibility data show that the compound is in the LS state in the temperature region 5–100 K ($\chi_m T$ = 0.39 cm^3 K mol^{-1}) and undergoes a very gradual thermal SCO upon further warming with $T_{1/2}$ = 270 K (Fig. 3). Such a gradual SCO is a typical phenomenon for a $[Co(terpy)_2]^{2+}$ salt. Further heating shows a discontinuity near 350 K. The $\chi_m T$ value continues to increase very slowly above 350 K, and reaches 2.29 cm^3 mol^{-1} K at 400 K which is identical to complete HS $[Co(terpy)_2]^{2+}$.

2.2. Spin-crossover cobalt(II) complexes with OH-terpy ligand

2,6-Bis(2-pyridyl)-4(1*H*)-pyridone can be coordinated to cobalt(II) ion in the enol form (OH-terpy ligand). Gaspar et al. reported on a new cobalt(II) SCO family $[Co(OH\text{-}terpy)_2]X_2{\cdot}nH_2O$ (X = SO_4^{2-}, n = 0; Cl^-, n = 1; ClO_4^-, n = 1) [63,64]. The single crystal structure of $[Co(OH\text{-}terpy)_2](ClO_4)_2{\cdot}H_2O$ (**3·H$_2$O**), is composed of discrete $[Co(OH\text{-}terpy)_2]^{2+}$cations, ClO_4^- anions, and a H_2O molecule. The tridentate OH-terpy ligand is coordinated in a *fac* fashion resulting in a tetragonally distorted $[CoN_6]$ octahedron. The axial Co–$N_{central}$ distances are considerably shorter than Co–N_{distal} distances occupying equatorial sites. The N–Co–N angles of each OH-terpy ligand also reflect that the 4-terpyridone ligand cannot form a precise octahedron because the bond angles are reduced from the ideal value of 180°. The water molecule is linked to two adjacent ClO_4^- by hydrogen bonding to form infinite chains and the cationic species are strongly attached to these chains. The OH group present in the central ring also interacts with the oxygen atom of the water molecule *via* hydrogen bonding. The magnetic behavior of **3·H$_2$O** displays strong temperature dependence leading to gradual SCO at 172 K (Fig. 4). The $\chi_m T$ value is equal to 0.4 cm^3 K mol^{-1} below 100 K corresponding with the LS state. On heating, the $\chi_m T$ value increases gradually until it reaches 2.48 cm^3 K mol^{-1} at 350 K.

The cobalt(II) compound $[Co(OH\text{-}terpy)_2](CF_3SO_3)_2{\cdot}H_2O$ (**4·H$_2$O**) displays both unique magnetic behavior and two kinds of polymorphs (Fig. 5) [65]. Polymorph 1 reveals a gradual SCO in the temperature region 300–120 K, whereas polymorph 2 exhibits

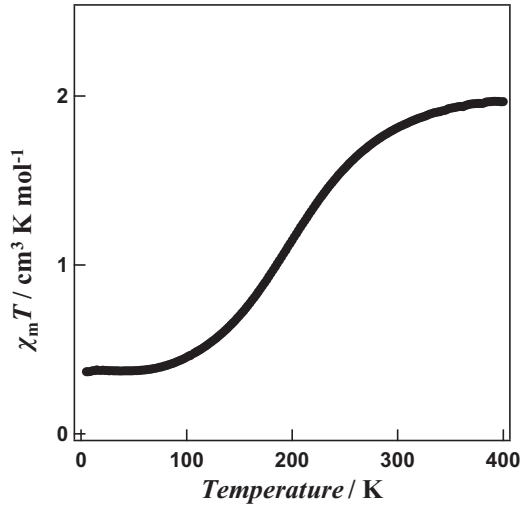

Fig. 2. Magnetic property for **1·0.5H$_2$O**.
Adapted from Ref. [60].

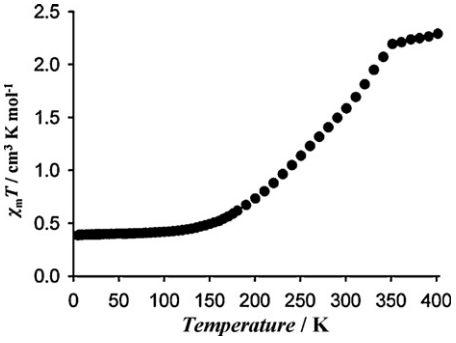

Fig. 3. Variable temperature magnetic susceptibility data for **2**.
Adapted from Ref. [62].

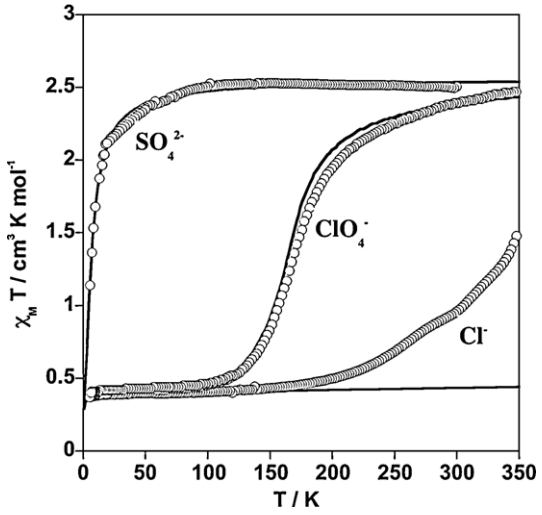

Fig. 4. Temperature dependence of the $\chi_m T$ product for compounds (**1**) [Co(OH-terpy)$_2$]SO$_4$, (**2**) [Co(OH-terpy)$_2$]Cl$_2$·H$_2$O and (**3**) **3·H$_2$O**.
Adapted from Ref. [63].

the onset of a continuous HS to LS conversion inducing an abrupt reverse spin transition in the temperature region 217–203 K. The unstable HS intermediate phase (IP) formed undergoes a general spin transition by strong a cooperative effect confirmed by a hysteresis loop of 33 K width. The structural analysis is indicative of further information for a crystallographic phase transition, which takes place concomitantly with the reverse spin transition.

3. Porous material with a spin-crossover cobalt(II) complex

Porous coordination polymers (PCPs) have drawn the attention of researchers because of their applicability in the field of gas storage, gas separation, and heterogeneous catalysis [66–72]. The SCO polymers have also led to functional frameworks, where the magnetic properties change in the presence or absence of guest molecules because they can modify the electronic environment of the metal centers [39,41,73]. Recently, iron(II) SCO PCPs with Hofmann-like or interpenetrated framework have been the subject of many studies [74,75]. The SCO compounds containing a microporous framework can lead to multifunction behavior such as thermo-, photo- and piezo-switching. For SCO cobalt(II) complexes, only one example of a 1-D SCO cobalt(II) PCP has been reported.

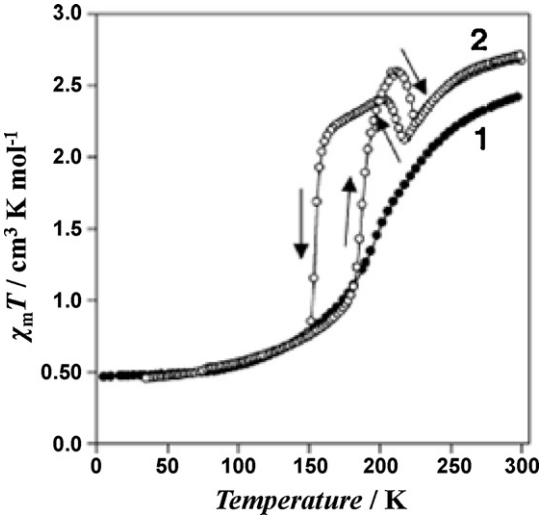

Fig. 5. $X_m T$ vereus T plot for polymorphs 1 (filled circles) and 2 (open circles) in **4·H$_2$O**.
Adapted from Ref. [65].

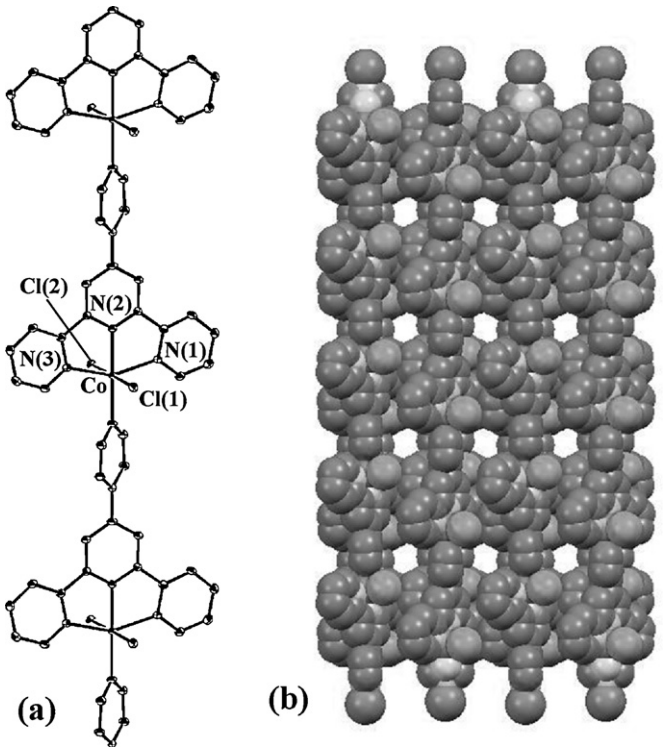

Fig. 6. (a) X-ray crystal structure of the directional 1-D network **5·MeOH** in 'head-to-tail' fashion. Hydrogen atoms and solvent molecules are omitted for clarity. (b) Space-filling view of the compound with the solvent molecules omitted.
Adapted from Ref. [76].

3.1. Spin-crossover cobalt(II) complex with the pyterpy ligand

The cobalt(II) complex, [Co(pyterpy)Cl$_2$]·MeOH (**5·MeOH**) was obtained by self-assembly of 4′-(4‴-pyridyl)-2,2′:6′,2″-terpyridine (pyterpy) and cobalt(II) chloride in MeOH [76]. The compound **5·MeOH** adopts monoclinic $P2/c$ space group at room temperature (Fig. 6). The bond lengths are consistent with those of typical HS cobalt(II) compounds. The complexation between terpy and py moieties appended to the pyterpy ligand and cobalt(II) chloride form a 1-D network. The two Cl^- anions occupy the two axial positions with Co–Cl distance of 2.4665(7) Å and Cl(1)–Co–Cl(2) angle of 179.02(3)°. The square base of the octahedron consists of one py and three py moieties in the terpy unit with Co–N(4) distance of 2.137(3) Å for the py unit and Co–N(2) distance of 2.067(3) Å for the central py of the terpy unit. The other two Co–N(1) and Co–N(3) distances are 2.185(2) Å. The N_{py}–Co–$N_{central}$ angle between terminal py and the central py moieties attached to the terpy unit is 180°, and the N_{distal}–Co–N_{distal} angle between the distal py in the terpy unit is 152°. The py and the terpy units are not coplanar but tilted by 50°. The 1-D networks align along the b axis. The 1-D framework formed by π–π stacking among the terpy units leads to a quasi 3-D network. The MeOH molecules are located in the interchain position of the quasi 3-D network and could be removed by heating the sample at 410 K. The water-solvated [Co(pyterpy)Cl$_2$]·2H$_2$O (**5·2H$_2$O**) was obtained under the saturated vapor atmosphere at room temperature. The $\chi_m T$ value for **5·MeOH** is equal to 2.74 cm^3 K mol^{-1} in the temperature range 150–300 K, which is in the range of values expected for the HS cobalt(II) ion (Fig. 7). The $\chi_m T$ value for **5·2H$_2$O** is equal to 2.80 cm^3 K mol^{-1} at 300 K, corresponding to HS cobalt(II) ions. As the temperature decreases from 300 K, the $\chi_m T$ product

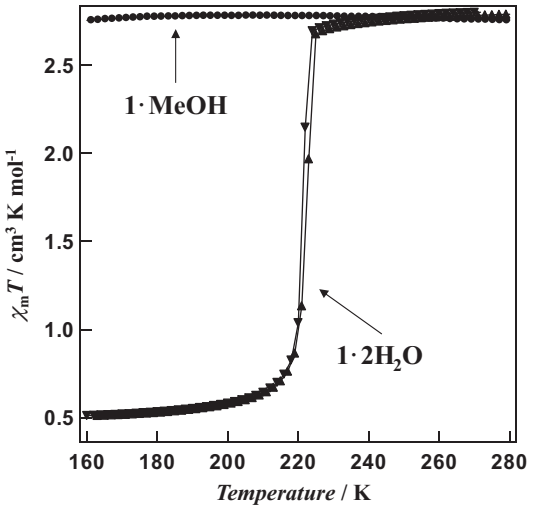

Fig. 7. $\chi_m T$ versus T plots for **5·MeOH** and **5·2H$_2$O**. Adapted from Ref. [76].

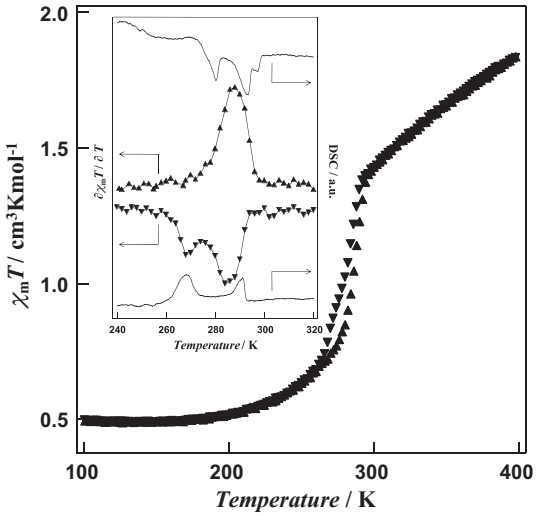

Fig. 9. $\chi_m T$ versus T plot (▲: heating mode, and ▼: cooling mode) for **6**. The insert graph shows the derivative $\partial\chi_m T/\partial T$ plot as a function of the temperature. Adapted from Ref. [92].

remained practically constant from 300 K to 225 K, then abruptly dropped around $T_{1/2}\downarrow$ = 222 K ($T_{1/2}\downarrow$ is defined as the inversion temperature at which there are 50% of HS and 50% of LS molecules in the cooling mode). At 150 K, the $\chi_m T$ value (0.41 cm^3 K mol^{-1}) shows that the spin transition from the HS to the LS state occurs (Fig. 10). Accordingly, this result suggests that the spin transition is directly related to the displacement of solvent molecules. On warming, the $\chi_m T$ value for **5·2H$_2$O** is almost constant from 5 K to 200 K, then abruptly increases at around $T_{1/2}\uparrow$ = 223 K, showing that the LS moieties is restored to the HS state with hysteresis loop (ΔT = 1 K) ($T_{1/2}\uparrow$ is defined as the inversion temperature at which there are 50% of HS and 50% of LS molecules in the warming mode, and ΔT is thermal hysteresis loop width). This is the only example of a 1-D SCO cobalt(II) PCP. The SCO behavior of the cobalt(II) complex **5·S** (S = solvent molecule) is dependent upon the guest molecules.

4. Soft material with spin-crossover cobalt(II) complexes

The soft materials are very interesting from the point of view not only of functional materials but in phase transitions [77–80]. Among these, transition metal complexes with liquid crystal properties called *metallomesogens* are important as molecular-based functional materials [81,82]. For instance, the metal complexes with the long alkyl chains exhibit a synchronicity between the central metal complexes and the long alkyl chains. Putting a cobalt(II) complex with SCO in the flexible and soft space formed by long alkyl chains is expected to show novel physical properties based on a synergy between SCO and response of the flexibility toward external stimuli [83–91].

4.1. Spin-crossover cobalt(II) complex with the C5C12C10-terpy ligand

The cobalt(II) compound [Co(C5C12C10-terpy)$_2$](BF$_4$)$_2$(6) (C5C12C10-terpy = 4′-5‴-decyl-1‴-heptadecyloxy-2,2′:6′,2″-terpyridine) with branched alkyl chains was obtained as brown powder by reaction of Co(BF$_4$)$_2$ and C5C12C10-terpy in MeOH [92]. The compound **6** shows both spin transition and crystal-mesophase transition. In this system, the branched alkyl chains play an important role not only decreasing the mesophase transition temperature but in the generation of synchronization between the liquid-crystal and spin transition temperatures in the compound. A rod-like geometry is proposed for the molecular structure of **6** by computer simulation (Fig. 8). The liquid-crystalline property for **6** was confirmed by powder X-ray diffraction (XRD), and polarizing optical microscopy (POM). The powder XRD patterns display a diffuse and broad scattering halo centered at 4.5 Å (2θ = 19.6°) in the wide-angle region, indicative of a liquid-like order of the aliphatic chains and thus of the fluid-like nature of the phase. In the small-angle region, the XRD pattern reveals three reflections in a ratio of 1:1/2:1/3:1/4, which can be indexed as the (0 0 1), (0 0 2), (0 0 3), and (0 0 4) reflections of a lamellar phase with a periodicity d = 23.9 Å (2θ = 4.0°). The typical fan-shaped texture is shown at 300 K in the natural texture. The mesophase was identified as a smectic A (SmA) mesophase based on the texture by POM and the powder XRD pattern.

The $\chi_m T$ value for **6** is equal to 0.50 cm^3 K mol^{-1} at 100 K, which is in accord with LS cobalt(II) ions (Fig. 9). On heating, the $\chi_m T$ product remained constant from 100 K to 200 K, then abruptly increased around $T_{1/2}\uparrow$ = 288 K. The $\chi_m T$ value at 400 K is 1.73 cm^3 K mol^{-1}, indicative of the spin transition from the LS to the HS state. On cool-

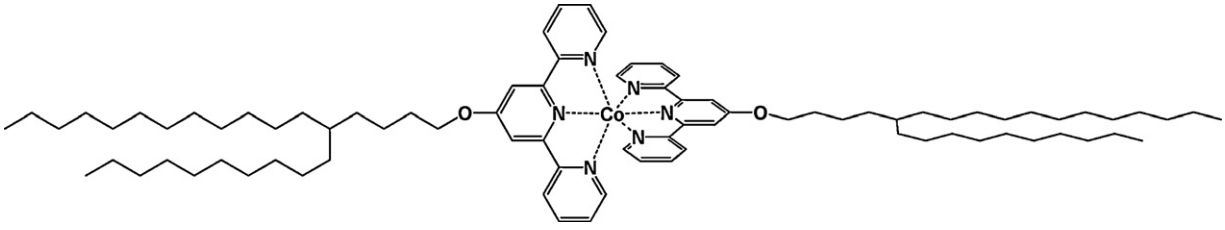

Fig. 8. Chemical structure of the cation in **6**.

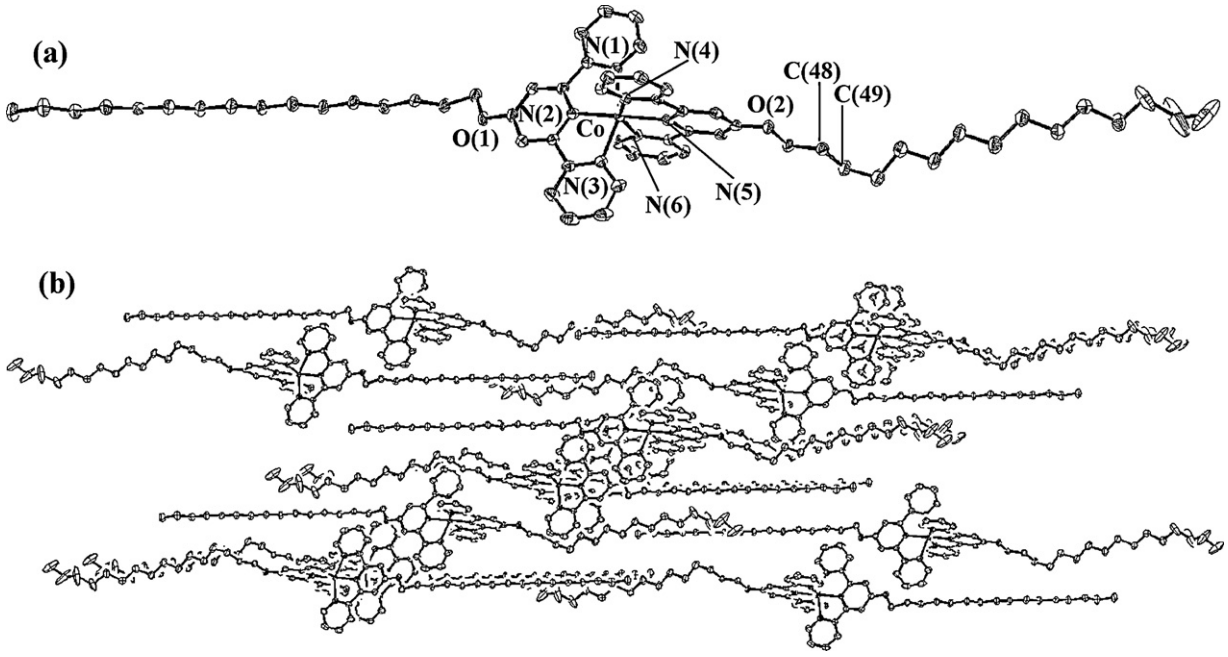

Fig. 10. (a) ORTEP drawing of cation of **7**·**MeOH** showing 50% probability displacement ellipsoids. (b) Projection of the crystal structure of cation of **7**·**MeOH** along the *bc* plane. BF_4^- anions, MeOH molecules and H atoms are omitted for clarity.
Adapted from Ref. [93].

ing, the $\chi_m T$ value for **6** decreases gradually from 400 K to 292 K, then abruptly drops at around $T_{1/2}\downarrow$ = 284 K. This demonstrates that the HS moieties are restored to the LS state with a hysteresis loop (ΔT = 4 K). Additional thermal cycles did not modify the thermal hysteresis loop.

The insert of Fig. 9 shows the maximum of the derivative $\partial\chi_m T/\partial T$ in the spin transition behavior and DSC curves measured at scan rate the same as magnetic measurement (2 K min^{-1}) for **6**. The maximum of the derivative $\partial\chi_m T/\partial T$ agrees with the peaks in DSC curves. On heating, the spin transition temperature was observed at 288 K, and the temperature is consistent with crystal-to-mesophase transition temperature from crystal to S_A phases. On the other hand, the maximum of the derivative $\partial\chi_m T/\partial T$ was observed at 268 K and 284 K on cooling, and the mesophase-to-crystal transitions occur in the same temperature range. These results reflect that the spin transition for **6** is triggered by a crystal-mesophase transition. Below 270 K, the compound **6** does not melt, and the Co–N bond distance in the LS state becomes short, while it melts on heating, and the spin transition from LS to HS states results in the elongation of the Co–N bond distance.

4.2. Spin-crossover cobalt(II) complex with C16-terpy ligand

The cobalt(II) compound $[Co(C16\text{-terpy})_2](BF_4)_2$·MeOH (**7**·**MeOH**) (C16-terpy is 4′-hexadecyloxy-2,2′:6′,2″-terpyridine) was obtained by reaction of $Co^{II}(BF_4)_2$ (1:2 metal-to-ligand molar ratio) with C16-terpyin methanol[93]. The single crystal X-ray analysis at 130 K, reveals that each of the cobalt(II) atoms is octahedrally coordinated to six nitrogen atoms from the two C16-terpy ligands, i.e. an N_6 donor set (Fig. 10). The Co–N bond lengths lie in the median value compared with those for typical LS and HS cobalt(II) compounds [2]. The average $Co–N_{central}$ distances (1.99 Å) are shorter than the $Co–N_{distal}$ distances (2.13 Å), which induces a pronounced distortion of the CoN_6 octahedron. Three pyridine rings in C16-terpy ligand exist in the co-plane, and the two tridentate C16-terpy ligands in the compound are nearly perpendicular to one another. The long alkyl chains $C_{16}H_{33}O$ which form a rod like structure are stuck out of 4′-position in the terpyridine moiety, exhibiting two modes within the lattice. One long alkyl chain with O(1) has is essentially straight, whereas the other chain with O(2) has twisted at the C(48)–C(49) location and is curved overall. The $[Co(C16\text{-terpy})_2]^{2+}$cations form short contacts (3.49 Å) through the side pyridine and nearest neighbor pyridine rings in the ligands on an *ab* plane, providing a 2-D sheet extended by the π–π interactions. Furthermore, there is a fastener effect between the chains which face each other in the complexes. The molecular packing of **7**·**MeOH** is very tight. This is suggestive of strong intermolecular interactions in the molecular assembly. The compound **7**·**MeOH** exhibits gradual SCO behavior in the temperature range 5–360 K (Fig. 11). The $\chi_m T$ value for **7**·**MeOH** gradually increases from 0.54 cm^3 K mol^{-1} to 1.83 cm^3 K mol^{-1} at 360 K, and then the $\chi_m T$ value decreases to 1.58 cm^3 K mol^{-1} at 400 K due to the removal of the MeOH molecules.

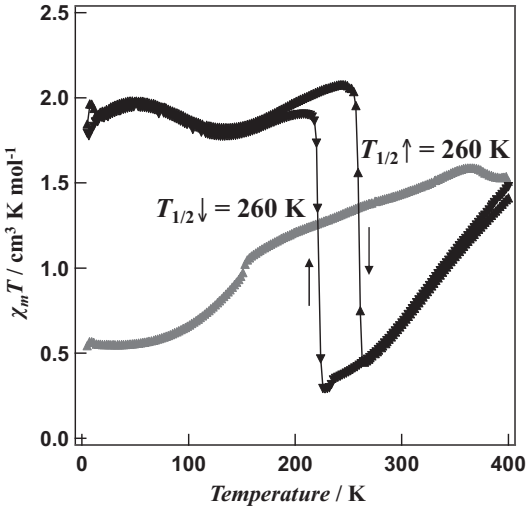

Fig. 11. $\chi_m T$ versus T plots for **7**·**MeOH** (▲) and **7** (▲: heating mode and ▼: cooling mode).
Adapted from Ref. [93].

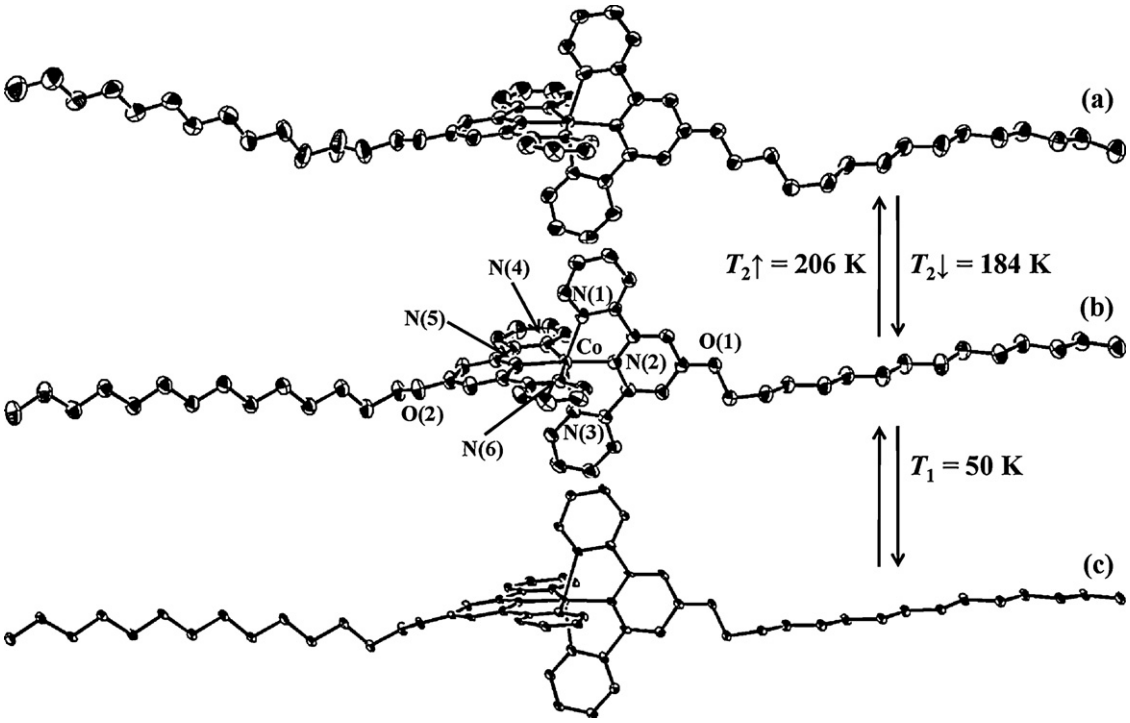

Fig. 12. ORTEP drawing of cation of **8**·**MeOH** showing 50% probability displacement ellipsoids. (a) HS2 phase at 190 K, (b) HS1 phase at 190 K, and (c) LS phase at 10 K. Adapted from Ref. [94].

The non-solvated compound $[Co(C16\text{-terpy})_2](BF_4)_2$ (**7**) was obtained by annealing **7**·**MeOH** at 400 K. The $\chi_m T$ value for the non-solvated compound **7** decreases gradually from 1.58 $cm^3\,K\,mol^{-1}$ at 400 K to 0.41 $cm^3\,K\,mol^{-1}$ at 226 K, showing normal thermal SCO behavior. Further cooling increases $\chi_m T$ abruptly at around $T_{1/2}\downarrow = 217$ K to 2.01 $cm^3\,K\,mol^{-1}$ at 206 K. On heating, the $\chi_m T$ value produces an undulation between 1.70 and 2.15 $cm^3\,K\,mol^{-1}$ in the temperature range from 5 K to 251 K. The undulated magnetic behavior is difficult to understand. However, it may be thought that it is caused by the structural changes. The powder XRD patterns also show that the structure at 50 K is different from that at 130 K. On further heating, $\chi_m T$ decreases steeply at around $T_{1/2}\uparrow = 260$ K, corresponding to the transition from HS to LS state. Then the $\chi_m T$ value gradually increases in the temperature range from 267 K to 400 K. In the additional cycle, the wide thermal hysteresis loop ($\Delta T = 43$ K) remains unchanged in successive thermal cycles. It is confirmed that the non-solvated compound **7** exhibits a "reverse spin transition" caused by a drastic phase transition involving a structural change in the long alkyl chain system.

4.3. Spin-crossover cobalt(II) complex with C14-terpy ligand

Single crystal X-ray analysis of the cobalt(II) compound $[Co(C14\text{-terpy})_2](BF_4)_2{\cdot}MeOH$ (**8**·**MeOH**) (C14-terpy is 4′-tetradecyloxy-2,2′:6′,2″-terpyridine) was successfully carried out in the HS1 and HS2 phases at 190 K and in LS phase at 10 K, which reveals that the central cobalt(II) atoms are coordinated to six nitrogen atoms of the two C14-terpy ligands in a distorted octahedral arrangement. The respective six Co–N distances have different lengths. The sample in the HS1 phase was isolated by heating to 190 K after cooling at 100 K. In the HS1 phase (Fig. 12(b)). The structure of **8**·**MeOH** is similar to that of **7**·**MeOH**. The bond lengths are typical of HS cobalt(II) compounds. The crystal structure of **8**·**MeOH** was also measured in the LS phase at 10 K (Fig. 12(c)). Although the molecular structures of the samples in LS and HS1 phases are almost the same, there is a unique difference in bond length. The $Co\text{–}N_{central}$ distance (1.88 Å) is much shorter than that of HS1 ($\Delta r_{HS1\text{–}LS} = 0.15$ Å). Two terpyunits are asymmetric, and the differences in the $Co\text{–}N_{distal}$ distances are evaluated between the N(1)∩N(3) and the N(4)∩N(6) terpyunits. The average Co–N distance of Co–N(1) and Co–N(3) is 2.13 Å ($\Delta r_{HS1\text{–}LS} = 0.02$ Å), and that of Co–N(4) and Co–N(6) is 1.98 Å ($\Delta r_{HS1\text{–}LS} = 0.16$ Å). The Co–N distance shrinks slightly in the N(1)∩N(3) terpyunit but considerably in the N(4)∩N(6) terpyunit. The distance between cobalt(II) ion and N(4)∩N(6) terpyunit shrinks accompanying HS1 ↔ LS SCO behavior because there are interchain interactions between the complexes. The sample in the HS2 phase was also isolated by cooling from room temperature to 190 K, and also measured (Fig. 12(a)). Although the molecular structures of the samples in HS1 and HS2 phases are almost the same, there is a crucial difference in the alkyl chain form. The chains curved in the HS2 phase, and the cations in the HS2 phase form a bent structure as a result. The $Co\text{–}N_{central}$ distance is 1.99 Å, and is shorter than that for HS1 ($\Delta r_{HS1\text{–}HS2} = 0.04$ Å). The $Co\text{–}N_{distal}$ distances vary between the N(1)∩N(3) and the N(4)∩N(6) terpyunits. The average Co–N distance in Co–N(1) and Co–N(3) is 2.14 Å ($\Delta r_{HS1\text{–}HS2} = 0.01$ Å), and that in Co–N(4) and Co–N(6) is 2.08 Å ($\Delta r_{HS1\text{–}HS2} = 0.07$ Å). The distance in the N(4)∩N(6) terpyunit is shorter than that in the N(1)∩N(3) terpy unit. The crystal structure reveals that the compound changes its structure around the cobalt(II) ion during HS1 ↔ HS2 conversion. The symmetry around cobalt(II) ion in the HS2 phase is better than that in the HS1 phase.

The compound **8**·**MeOH** exhibited unique magnetic behavior in the temperature range of 5–300 K (Fig. 13). **8**·**MeOH** shows SCO behavior and phase transition, and SCO temperature without thermal hysteresis and phase transition temperature with thermal hysteresis expressed as T_1 and $T_2\uparrow$ and $T_2\downarrow$, respectively. The magnetic properties show that the value of $\chi_m T$ for **8**·**MeOH** at 5 K is equal to 0.43 $cm^3\,K\,mol^{-1}$, which corresponds to that expected for the LS state in cobalt(II) compounds. On heating, the $\chi_m T$ value increased steeply around $T_1 = 50$ K. The $\chi_m T$ value at 100 K is equal to 3.62 $cm^3\,K\,mol^{-1}$, representing the HS state. Further heating leads to an abrupt drop in the $\chi_m T$ value around $T_2\uparrow = 206$ K. The

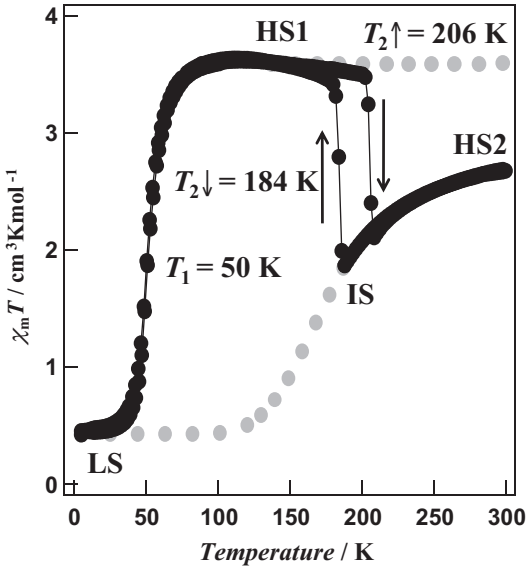

Fig. 13. Magnetic susceptibility measurement displaying spin crossover and incomplete spin transition for **8**·**MeOH**. See text for explanation of gray and black data. Adapted from Ref. [94].

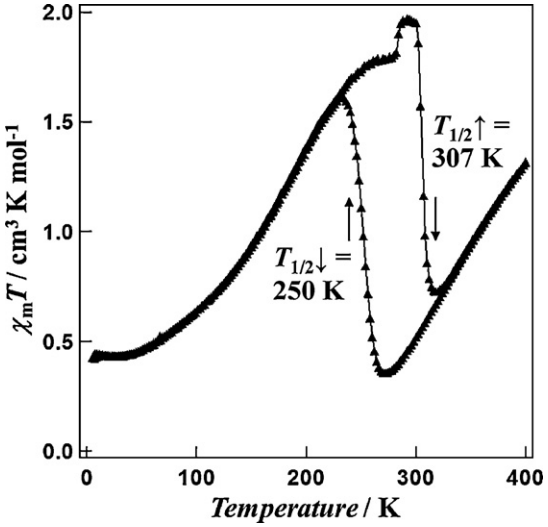

Fig. 14. $\chi_m T$ versus T plots for **8** (▲: heating mode and ▼: cooling mode). Adapted from Ref. [93].

$\chi_m T$ value at 210 K is equal to 2.11 cm^3 K mol^{-1}. On cooling, the $\chi_m T$ value increases abruptly around $T_2\downarrow$ = 184 K, and is equal to 3.32 cm^3 K mol^{-1} at 182 K. In the HS1 ↔ HS2 transition, a thermal hysteresis loop ΔT = 22 K was observed. The unique magnetic behavior and the thermal hysteresis loop remains unchanged even after successive heating and cooling. The fairly abrupt conversion of $\chi_m T$ with a hysteresis loop is indicative of a strong cooperative interaction. On further cooling, the $\chi_m T$ value decreases steeply around T_1 = 50 K and returns to the LS state (0.43 cm^3 K mol^{-1}) at 5 K. No hysteresis loop was noted in the SCO at 50 K. Therefore, the cobalt(II) compound **8**·**MeOH** exhibits SCO at T_1 = 50 K without hysteresis, and HS1 ↔ HS2 transition at $T_2\uparrow$ = 206 K and $T_2\downarrow$ = 184 K with hysteresis. The unique magnetic property can be explained as following. There are two HS states, HS1 and HS2, in the cobalt(II) compound (Fig. 13). One shows steep SCO behavior ($T_{1/2}$ = 50 K), and the other shows gradual SCO behavior ($T_{1/2}$ = 175 K) as shown by gray plots. With the structural phase transition occurring at $T_2\uparrow$ = 206 K and $T_2\downarrow$ = 184 K induced by the motion of the long alkyl chains, the magnetic behavior of **8**·**MeOH** is shown by the black plots.

The non-solvated compound [Co(C14-terpy)$_2$](BF$_4$)$_2$ (**8**) was obtained by annealing **8**·**MeOH** at 400 K. The compound **8** also exhibited a "reverse spin transition" (Fig. 14.) [93]. The $\chi_m T$ value for **8** gradually decreases from 1.57 cm^3 K mol^{-1} at 400 K to 0.52 cm^3 K mol^{-1} at 268 K, and then abruptly increases at around $T_{1/2}\downarrow$ = 250 K to 1.73 cm^3 K mol^{-1} at 230 K. Compound **8** exhibits a "reverse spin transition" phenomenon from LS state to HS state on cooling. On further cooling, $\chi_m T$ value gradually decreases to 0.44 cm^3 K mol^{-1} at 5 K, which follows normal SCO behavior. On heating, $\chi_m T$ value gradually increases to 1.96 cm^3 K mol^{-1} at 280 K, and a $\chi_m T$ jump from 1.96 cm^3 K mol^{-1} to 2.15 cm^3 K mol^{-1} was observed at 298 K. On further heating, $\chi_m T$ value abruptly decreases, which shows the feature of "reverse spin transition" from HS to LS state at $T_{1/2}\uparrow$ = 307 K to 0.95 cm^3 K mol^{-1} at 320 K. Then the $\chi_m T$ value gradually increases up to 400 K. In the additional cycle, the thermal hysteresis loop (ΔT = 57 K) remains unchanged in the successive thermal cycle, Thus compound **8** exhibits a "reverse spin transition". More importantly there is the wide hysteresis loop of 57 K which includes room temperature.

4.4. Spin-crossover cobalt(II) complex with C12-terpy ligand

The solvated cobalt(II) compound [Co(C12-terpy)$_2$](BF$_4$)$_2$·EtOH·0.5H$_2$O (**9**·**EtOH**·**0.5H$_2$O**) (C12-terpy is 4′-dodecyloxy-2,2′:6′,2″-terpyridine) was obtained as a brown orange single crystal by slow recrystallization from EtOH solvent[95]. The single crystal structure of **9**·**EtOH**·**0.5H$_2$O** is similar to those of **7**·**MeOH** or **8**·**MeOH**, and **9**·**EtOH**·**0.5H$_2$O** also exhibits unique SCO behavior (Fig. 15). The $\chi_m T$ value for **9**·**EtOH**·**0.5H$_2$O** is 1.90 cm^3 K mol^{-1} at 5 K, and decreases to 0.93 cm^3 K mol^{-1} at 69 K on heating($T_{1/2}$ = 49 K). Upon further heating, the $\chi_m T$ value gradually increases to 2.03 cm^3 K mol^{-1} at 300 K ($T_{1/2}$ = 128 K). In the cooling mode, the magnetic behavior is almost equal to heating mode without thermal hysteresis. In other words, the magnetic behavior of **9**·**EtOH**·**0.5H$_2$O** shows "re-entrant SCO".

The non-solvated compound [Co(C12-terpy)$_2$](BF$_4$)$_2$ (**9**) was obtained by annealing **9**·**EtOH**·**0.5H$_2$O** at 400 K. The compound **9** also exhibits unique magnetic behavior (Fig. 16). The $\chi_m T$ value is 1.33 cm^3 K mol^{-1} at 5 K, and abruptly decreases to 0.64 cm^3 K mol^{-1} at 59 K on heating ($T_{1/2}$ = 49 K, and i in Fig. 16). On further heating, the $\chi_m T$ value gradually increases to 2.02 cm^3 K mol^{-1} at 265 K (ii

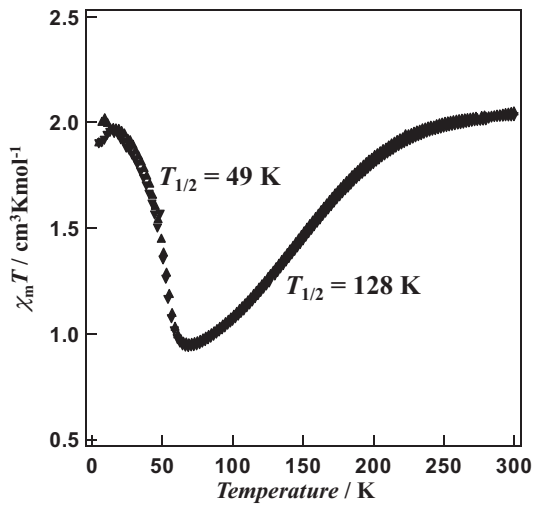

Fig. 15. $\chi_m T$ versus T plot for **9**·**EtOH**·**0.5H$_2$O**. Adapted from Ref. [95].

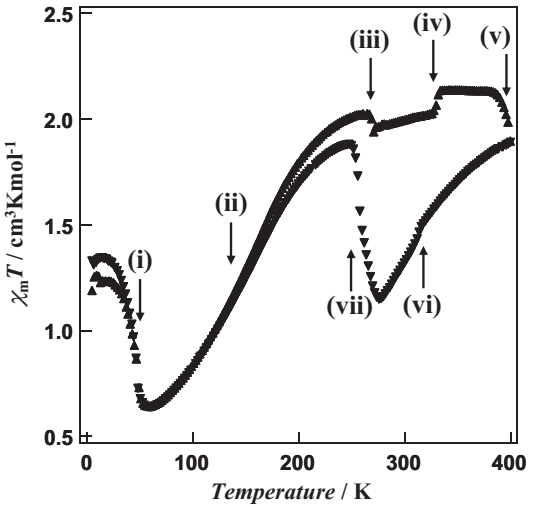

Fig. 16. $\chi_m T$ versus T plots for **9**. The multi phase transitions were observed at the points (i) at 49 K, (ii) at 160 K, (iii) at 269 K, (iv) at 330 K, (v) at around 400 K, (vi) at 314 K and (vii) at 258 K in the temperature range of 5–400 K.
Adapted from Ref. [95].

in Fig. 16), and two $\chi_m T$ jumps at 269 K and 330 K were observed (iii and iv in Fig. 16). On further heating, the $\chi_m T$ value is constant (2.14 cm^3 K mol^{-1}) between 334 K and 382 K, and abruptly drops at around 400 K (v in Fig. 16). On the other hand, the $\chi_m T$ value gradually decreases from 1.89 cm^3 K mol^{-1} at 400 K to 1.15 cm^3 K mol^{-1} at 276 K (vi in Fig. 16), and abruptly increases at $T_{1/2}\downarrow = 258$ K on cooling (vii in Fig. 16). On further cooling, the $\chi_m T$ value traces the heating line without thermal hysteresis. Upon additional heating and cooling, the unusual magnetic curve remains unchanged in the successive thermal cycles. The $\chi_m T$ change in the temperature range of 60–250 K can be assigned to normal SCO behavior. On the other hand, the SCO at $T_{1/2} = 49$ K, and spin transition at$T_{1/2}\uparrow \geq 400$ K and $T_{1/2}\downarrow = 258$ K can be assigned to "re-entrant SCO" and "reverse spin transition" behavior. The "reverse spin transition" at higher temperature also shows a very wide thermal hysteresis loop ($\Delta T \geq 142$ K), and room temperature located within the hysteresis loop.

5. Conclusion

In this review, we have described the magnetic properties and the structural characteristics of several SCO cobalt(II) complexes with terpy derivatives possessing various substituents at the 4-position. The substitution of the 4-position in the skeleton of terpy ligand allows diverse magnetic behavior of cobalt(II) complexes by enhancing intermolecular interactions in the solid state. Moreover, the interaction between other molecules from the outside and terpy-appended cobalt(II) complexes also influences their magnetic property. The $[Co(terpy)_2]X_2 \cdot nH_2O$ (**1·0.5H$_2$O** and **2**) and $[Co(OH\text{-}terpy)_2]X_2 \cdot nH_2O$ (**3·H$_2$O** and **4·H$_2$O**) exhibited gradual SCO behavior, whereas $[Co(pyterpy)Cl_2]\cdot S$ (**5·S**) showed SCO depending on the guest solvent molecules involved. The $[Co(C5C12C10\text{-}terpy)_2](BF_4)_2$ (**6**) with branched alkyl chains exhibited SCO which was accompanied by liquid crystal transition. The $[Co(C_n\text{-}terpy)_2](BF_4)_2$(**7·MeOH** and **7**, **8·MeOH** and **8**, **9·EtOH·0.5H$_2$O** and **9**) with long alkyl chains showed unique SCO behavior namely "reverse spin transition" or "re-entrant SCO". From the aforementioned results, we believe that novel physical properties may be discovered in these metal complexes through coupling between the motion of flexible alkyl chains and the electronic states. These compounds with bistability are important as a means to develop novel switchable molecular devices in the future.

Acknowledgments

We would like to thank our numerous collaborators, whose contributions have been cited in this review. We also thank the financial support of the Grant-in-Aids for Science Research (No. 20350028) from the Ministry of Education, Culture, Sports, Science and Technology of the Japanese Government and for Priority Area "Coordination Programming" (area 2107) from the MEXT of Japan. Y.H.L. was also supported by the JSPS program of Postdoctoral Fellowships for Foreign Researchers (No. 2200341).

References

[1] L. Cambi, L. Szego, Chem. Ber. Dtsch. Ges. 64 (1931) 2591.
[2] P. Gütlich, H.A. Goodwin (Eds.), Spin Crossover in Transition Metal Compounds, vols. 233–235, Top. Curr. Chem., 2004.
[3] P. Gütlich, A. Hauser, H. Spiering, Angew. Chem., Int. Ed. Engl. 33 (1994) 2024.
[4] M. Nihei, T. Shiga, Y. Maeda, H. Oshio, Coord. Chem. Rev. 251 (2007) 2606.
[5] M.A. Halcrow, Coord. Chem. Rev. 253 (2009) 2493.
[6] Y. Sunatsuki, R. Kawamoto, K. Fujita, H. Maruyama, T. Suzuki, H. Ishida, M. Kojima, S. Iijima, N. Matsumoto, Coord. Chem. Rev. 254 (2010) 1871.
[7] J.A. Real, A.B. Gaspar, V. Niel, M.C. Muñoz, Coord. Chem. Rev. 236 (2003) 121.
[8] H. Toftlund, Coord. Chem. Rev. 94 (1989) 67.
[9] H.A. Goodwin, Coord. Chem. Rev. 18 (1976) 293.
[10] P. Gütlich, Struct. Bond. (Berlin) 44 (1981) 83.
[11] E. König, G. Ritter, S.K. Kulshreshtha, Chem. Rev. 85 (1985) 219.
[12] R.C. Stoufer, D.H. Busch, W.B. Hadley, J. Am. Chem. Soc. 83 (1961) 3732.
[13] R. Hogg, R.G. Wilkins, J. Chem. Soc. (1962) 341.
[14] P.G. Sim, E. Sinn, J. Am. Chem. Soc. 103 (1981) 241.
[15] D. Cozak, F. Gauvin, J. Demers, Can. J. Chem. 64 (1986) 71.
[16] D.M. Halepoto, D.G.L. Holt, L.F. Larkworthy, G.L. Leigh, D.C. Povey, G.W. Smith, J. Chem. Soc., Chem. Comm. (1989) 1322.
[17] A.K. Hughes, V.J. Murphy, D. O'Hare, J. Chem. Soc., Chem. Comm. 2 (1994) 163.
[18] W. Kläui, J. Chem. Soc., Chem. Comm. 700 (1979).
[19] M.G. Simmons, L.J. Wilson, Inorg. Chem. 22 (1983) 2527.
[20] A. Earnshaw, P.C. Hewlett, E.A. King, L.F. Larkworthy, J. Chem. Soc. A (1968) 241.
[21] L.G. Marzilli, P.A. Marzilli, Inorg. Chem. 11 (1972) 457.
[22] J. Zarembowitch, N. J. Chem. 16 (1992) 255.
[23] J. Zarembowitch, O. Kahn, Inorg. Chem. 23 (1984) 589.
[24] S. Brooker, J. de, G. Duncan, R.J. Kelly, P.G. Plieger, B. Moubaraki, K.S. Murray, G.B. Jameson, J. Chem. Soc., Dalton Trans. (2002) 2080.
[25] L. Sacconi, Coord. Chem. Rev. 8 (1972) 351.
[26] M.M. Rohmer, A. Strich, M. Bénard, J.P. Malrieu, J. Am. Chem. Soc. 123 (2001) 9126.
[27] R. Clérac, F.A. Cotton, K.R. Dunbar, T. Lu, C.A. Murillo, X. Wang, J. Am. Chem. Soc. 122 (2000) 2272.
[28] W. Vreugdenhill, J.H. van Diemen, R.A.G. de Graaff, J.G. Haasnoot, J. Reedijk, A.M. van der Kraan, O. Kahn, J. Zarembowitch, Polyhedron 9 (1990) 2971.
[29] J. Kröber, E. Codjovi, O. Kahn, F. Grolibre, C. Jay, J. Am. Chem. Soc. 115 (1993) 9810.
[30] O. Sato, T. Iyoda, A. Fujishima, K. Hashimoto, Science 272 (1996) 704.
[31] V. Niel, J.M. Martínez-Agudo, M.C. Muñoz, A.B. Gaspar, J.A. Real, Inorg. Chem. 40 (2001) 3838.
[32] J.-F. Létard, P. Guionneau, O. Nguyen, J.S. Costa, S. Marcen, G. Chastanet, M. Marchivie, L. Goux-Capes, Chem. Eur. J. 11 (2005) 4582.
[33] W. Kosaka, K. Nomura, K. Hashimoto, S. Ohkoshi, J. Am. Chem. Soc. 127 (2005) 8590.
[34] J.A. Real, B. Gallois, T. Granier, F. Suez-Panama, J. Zarembowitch, Inorg. Chem. 31 (1992) 4972.
[35] B. Gallois, J.A. Real, C. Hauw, J. Zarembovitch, Inorg. Chem. 29 (1990) 1152.
[36] Z.J. Zhong, J. Tao, Z. Yu, C. Dun, Y. Liu, X. You, J. Chem. Soc., Dalton Trans. (1988) 327.
[37] J.G. Haasnoot, G. Vos, W.L. Groeneveld, Z. Naturforsch., Teil B 32 (1977) 1421.
[38] W. Vreugdenhil, J.G. Haasnoot, O. Kahn, P. Thuéry, J. Reedijk, J. Am. Chem. Soc. 109 (1987) 5272.
[39] J.A. Real, E. Andrés, M.C. Muñoz, M. Julve, T. Granier, A. Bousseksou, F. Varret, Science 268 (1995) 265.
[40] N. Moliner, M.C. Muñoz, S. Létard, X. Solans, N. Menéndez, A. Goujon, F. Varret, J.A. Real, Inorg. Chem. 39 (2000) 5390.
[41] G.J. Halder, C.J. Kepert, B. Moubaraki, K.S. Murray, J.D. Cashion, Science 298 (2002) 1762.
[42] Y. Garcia, O. Kahn, L. Rabardel, B. Chansou, L. Salmon, J.P. Tuchagues, Inorg. Chem. 38 (1999) 4663.
[43] D. Chernyshov, M. Hostettler, K.W. Törnroos, H.B. Bürgi, Angew. Chem., Int. Ed. 42 (2003) 3825.
[44] T. Kitazawa, Y. Gomi, M. Takahashi, M. Takeda, M. Enomoto, A. Miyazaki, T. Enoki, J. Mater. Chem. 6 (1996) 119.
[45] V. Niel, J.M. Martinez-Agudo, M.C. Muñoz, A.B. Gaspar, J.A. Real, Inorg. Chem. 40 (2001) 3838.
[46] A. Galet, V. Niel, M.C. Muñoz, J.A. Real, J. Am. Chem. Soc. 125 (2003) 14224.
[47] S. Hayami, Z.Z. Gu, M. Shiro, Y. Einaga, A. Fujishima, O. Sato, J. Am. Chem. Soc. 122 (2000) 7126.

[48] S. Hayami, Z.Z. Gu, H. Yoshiki, A. Fujishima, O. Sato, J. Am. Chem. Soc. 123 (2001) 11644.
[49] J.F. Létard, P. Guionneau, E. Codjovi, O. Lavastre, G. Bravic, D. Chasseau, O. Kahn, J. Am. Chem. Soc. 119 (1997) 10861.
[50] C.L. Xie, D.N. Hendrickson, J. Am. Chem. Soc. 109 (1987) 6981.
[51] A.J. Conti, C.-L. Xie, D.N. Hendrickson, J. Am. Chem. Soc. 111 (1989) 1171.
[52] A. Hauser, J. Adler, P. Gütlich, Chem. Phys. Lett. 152 (1988) 468.
[53] J.G. Schmidt, W.S. Brey, R.C. Stoufer, Inorg. Chem. 6 (1967) 268.
[54] S. Kremer, W. Henke, D. Reinen, Inorg. Chem. 21 (1982) 3013.
[55] C.M. Harris, T.N. Lockyer, R.L. Martin, H.R.H. Patil, E. Sinn, I.M. Stewart, Aust. J. Chem. 22 (1969) 2105.
[56] J.S. Judge, W.A. Baker, Inorg. Chim. Acta 1 (1967) 68.
[57] E.N. Maslen, C.L. Raston, A.H. White, J. Chem. Soc. (1974) 1803.
[58] B.N. Figgis, E.S. Kucharski, A.H. White, Aust. J. Chem. 36 (1983) 1527.
[59] R.C. Stoufer, D.W. Smith, E.A. Clevenger, T.E. Norris, Inorg. Chem. 5 (1966) 1167.
[60] H. Oshio, H. Spiering, V. Ksenofontov, F. Renz, P. Gütlich, Inorg. Chem. 40 (2001) 1143.
[61] B.N. Figgis, E.S. Kucharski, A.H. White, Aust. J. Chem. 36 (1983) 1537.
[62] C.A. Kilner, M.A. Halcrow, Dalton Trans. 39 (2010) 9008.
[63] A.B. Gaspar, M.C. Muñoz, V. Niel, J.A. Real, Inorg. Chem. 40 (2001) 9.
[64] A. Galet, A.B. Gaspar, M.C. Muñoz, J.A. Real, Inorg. Chem. 45 (2006) 4413.
[65] G. Agustí, C. Bartual, V. Martínez, F.J. Muñoz-Lara, A.B. Gaspar, M.C. Muñoz, J.A. Real, N. J. Chem. 33 (2009) 1262.
[66] G. Férey, C. Mellot-Draznieks, C. Serre, F. Millange, Acc. Chem. Res. 38 (2005) 217.
[67] N.W. Ockwig, O. Delgado-Friedrichs, M. O_Keeffe, O.M. Yaghi, Acc. Chem. Res. 38 (2005) 176.
[68] S. Kitagawa, R. Kitaura, S. Noro, Angew. Chem. Int. Ed. 43 (2004) 2334.
[69] M.J. Rosseinsky, Micropor. Mesopor. Mater. 73 (2004) 15.
[70] C. Janiak, Dalton Trans. (2003) 2781.
[71] G.S. Papaefstathiou, L.R. MacGillivary, Coord. Chem. Rev. 246 (2003) 169.
[72] B. Moulton, M.J. Zaworotko, Chem. Rev. 101 (2001) 1629.
[73] S.M. Neville, G.J. Halder, K.W. Chapman, M.B. Duriska, P.D. Southon, J.D. Cashion, J.F. Létard, B. Moubaraki, K.S. Murray, C.J. Kepert, J. Am. Chem. Soc. 130 (2008) 2869.
[74] M. Ohba, K. Yoneda, G. Agustí, M.C. Muñoz, A.B. Gaspar, J.A. Real, M. Yamasaki, H. Ando, Y. Nakao, S. Sakaki, S. Kitagawa, Angew. Chem. Int. Ed. 48 (2009) 4767.
[75] G. Agustí, R. Ohtani, K. Yoneda, A.B. Gaspar, M. Ohba, J.F. Sánchez-Royo, M.C. Muñoz, S. Kitagawa, J.A. Real, Angew. Chem. Int. Ed. 48 (2009) 8944.
[76] S. Hayami, K. Hashiguchi, G. Juhász, M. Ohba, H. Okawa, Y. Maeda, K. Kato, K. Osaka, M. Takata, K. Inoue, Inorg. Chem. 43 (2004) 4124.
[77] S. Cobo, G. Molnár, J.A. Real, A. Bousseksou, Angew. Chem., Int. Ed. 45 (2006) 5786.
[78] J.F. Létard, O. Nouyen, H. Soyer, C. Mingotaud, P. Delhaès, O. Kahn, Inorg. Chem. 38 (1999) 3020.
[79] K. Kuroiwa, T. Shibata, A. Takada, N. Nemoto, N. Kimizuka, J. Am. Chem. Soc. 126 (2004) 2016.
[80] N.Y. Ha, Y. Ohtsuka, S.M. Jeong, S. Nishimura, G. Suzaki, Y. Takanishi, K. Ishikawa, H. Takezoe, Nat. Mater. 7 (2008) 43.
[81] M. Seredyuk, A.B. Gaspar, V. Ksenofontov, Y. Galyametdinov, J. Kusz, P. Gütlich, J. Am. Chem. Soc. 130 (2008) 1431.
[82] D. Kiriya, H.C. Chang, S. Kitagawa, J. Am. Chem. Soc. 130 (2008) 5515.
[83] Y. Galyametdinov, V. Ksenofontov, A. Prosvirin, I. Ovchinnikov, G. Ivanova, P. Gütlich, W. Haase, Angew. Chem., Int. Ed 40 (2001) 4269.
[84] S. Hayami, K. Danjobara, K. Inoue, Y. Ogawa, N. Matsumoto, Y. Maeda, Adv. Mater. 16 (2004) 869.
[85] S. Hayami, N. Motokawa, A. Shuto, N. Masuhara, T. Someya, Y. Ogawa, K. Inoue, Y. Maeda, Inorg. Chem. 46 (2007) 1789.
[86] T. Fujigaya, D.L. Jiang, T. Aida, J. Am. Chem. Soc. 125 (2003) 14690.
[87] T. Fujigaya, D.L. Jiang, T. Aida, J. Am. Chem. Soc. 127 (2005) 5484.
[88] J.A. Real, A.B. Gaspar, V.M. Niel, C. Muñoz, Coord. Chem. Rev. 236 (2003) 121.
[89] J.A. Real, A.B. Gaspar, M.C. Muñoz, Dalton Trans. (2005) 2062.
[90] M. Seredyuk, A.B. Gaspar, V. Ksenofontov, S. Reiman, Y. Galyametdinov, W. Haase, E. Rentschler, M.P. Gütlich, Chem. Mater. 18 (2006) 2513.
[91] Y. Bodenthin, U. Pietsch, H. Möhwald, D.G. Kurth, J. Am. Chem. Soc. 127 (2005) 3110.
[92] S. Hayami, R. Moriyama, A. Shuto, Y. Maeda, K. Ohta, K. Inoue, Inorg. Chem. 46 (2007) 7692.
[93] S. Hayami, Y. Shigeyoshi, M. Akita, K. Inoue, K. Kato, K. Osaka, M. Takata, R. Kawajiri, T. Mitani, Y. Maeda, Angew. Chem. Int. Ed. 44 (2005) 4899.
[94] S. Hayami, K. Murata, D. Urakami, Y. Kojima, M. Akita, K. Inoue, Chem. Commun. (2008) 6510.
[95] S. Hayami, K. Kato, Y. Komatsu, A. Fuyuhiro, M. Ohba, Dalton Trans. 40 (2011) 2167.